EPJ Web of Conferences **272**, 01010 (2022) https://doi.org/10.1051/epjconf/202227201010
QENS/WINS 2022

Controlling terahertz sound propagation: some preliminary Inelastic X-Ray Scattering result

Scott T. Lynch[1], *Alessio* De Francesco[2,*], *Luisa* Scaccia[3], and *Alessandro* Cunsolo[1]

[1]Department of Physics, University of Wisconsin at Madison, 1150 University Avenue, Madison, WI, USA
[2]CNR-IOM & INSIDE@ILL c/o Operative Group in Grenoble (OGG), F-38042 and Institut Laue Langevin, Grenoble, France
[3]Dipartimento di Economia e Diritto, Università di Macerata, Via Crescimbeni 20, 62100 Macerata, Italy

Abstract. The control of sound propagation in materials via the design of their elastic properties is an exciting task at the forefront of Condensed Matter. It becomes especially compelling at terahertz frequencies, where phonons are the primary conveyors of heat flow. Despite the increasing focus on this goal, this field of research is still in its infancy. To achieve a few advances in this field, we performed several Inelastic X-Ray Scattering (IXS) measurements on elementary systems as dilute suspensions of nanoparticles (NPs) in liquids. We found that nanoparticles can effectively impact the sound propagation of the hosting liquid. We also explored the possibility of shaping terahertz sound propagation in a liquid upon confinement on quasi-unidimensional cavities. These results are here reviewed and discussed, and future research directions are finally outlined.

1 Introduction

The control of sound propagation through the design of a material's structure is a long-term objective of a relevant portion of Condensed Matter physicists. In particular, achieving this goal at terahertz frequencies, where phonons are the leading heat carriers in insulators, will pave new avenues for developing novel thermal devices [1]. Furthermore, it will promote a transformation of the core activity of researchers: from the mere observation and formalization of a physical phenomenon - sound propagation - to its active steering via the engineering of novel artificial materials. Especially promising appears the capability of structuring nanoscale structures to function as the so-called phononic crystals (PCs). These devices are ideal candidates for implementing acoustic manipulation thanks to their mass and elastic modulus distributions with periodicity suited to impact the propagation of sound waves of specific frequencies, slowing it down, reflecting, or even stopping them [2]. Overall, PCs proved to be critical to the development of novel thermal devices, such as thermal diodes [3], thermoelectrics [4], and thermocrystals [5], and applications as relevant as energy harvesting [6], and management of thermal properties [7].

A prerogative of these devices is the ability to forbid acoustic propagation in some frequency bands, customarily referred to as phononic gaps, representing the mechanical equivalent of electronic and photonic bandgaps in semiconductors and photonic crystals, respectively. While in photonic crystals, band gaps originate from periodic variations of the refractive index, in PCs, they stem from the periodic modulation of density and elastic modulus. Inelastic X-Ray (IXS) [8, 9] and Neutron Scattering (INS) [10, 11] are the best-suited techniques to characterize the propagation of terahertz sound mode, via their direct access to the spectrum of density fluctuations in disordered systems or the phonon spectrum from crystalline materials. An alternative pathway to control terahertz acoustic propagation is to reduce acoustic lifetime by controlling the amount of disorder in the system. To understand this point, one may recognize that at sufficiently short distances and timescales - as well as at low temperatures – the dominant contribution to sound damping derives from either: 1) the inherent disorder of the liquid structure, *i.e.* the coexistence of a finite distribution of first neighboring atomic distances, and 2) the orientational component of the disorder, arising from the random orientation of locally ordered microdomains, similar to that of polycrystalline materials [12, 13]. The quasi-continuous distribution of local lattice parameters prevents density fluctuations from propagating with a well-defined sound velocity but rather with a range of propagation velocities; hence, the dominant sound mode spreads over a continuous superposition of eigenmodes. The mutual interference between these modes substantially damps acoustic propagation, causing a visible broadening of the collective excitations in the measured inelastic spectrum. These arguments suggest that the structural disorder impacts sound propagation, highlighting the possibility of manipulating the acoustic properties of a fluid by including randomly arranged structural heterogeneities. Indeed, the immersion of nanoparticles can substantially affect the fluid ability to support terahertz collective modes propagation [14]. Despite the undoubted scientific relevance, *IXS* and *INS* studies on these systems are still sporadic, partially owing to the challenging interpretation of the often unstructured

*e-mail: defrance@ill.fr

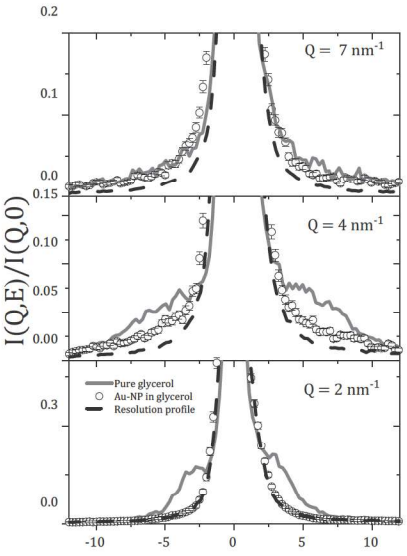

Figure 1. Selected *IXS* spectral shapes measured on a dilute suspension of Au nanorods in water at the Q values indicated. Data are from Ref. 14. Experimental spectra (open circles) are compared with their counterparts in the pure solvent (grey line) and the resolution function. All spectral profiles are normalized to their maxima for the sake of comparison.

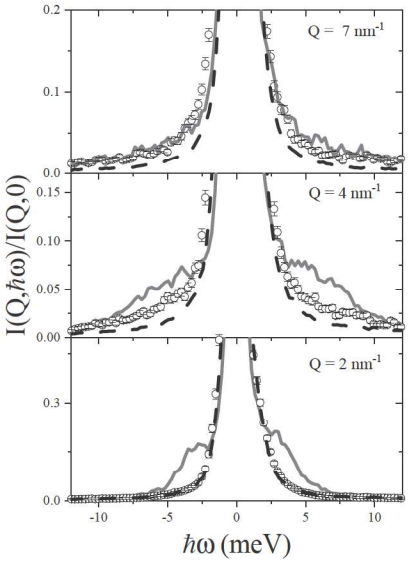

Figure 2. As in figure 1, but referring to a gold nanoparticle (AuNP) suspension in glycerol. Data are again from Ref. 14.

spectral profile, especially considering the lack of firm theoretical predictions of the spectral shape of complex materials. In several recent works, we showed how some of these inherent difficulties could be successfully addressed by using Bayesian inferential methods [15–17] enabling hypothesis tests, which might establish *e.g.* the number of inelastic modes most likely to appear in the spectrum, or even the most plausible analytical function describing measured lineshapes on a sound probabilistic basis. This paper briefly reviews some relevant results emerging from these studies.

2 The damping effect of nanoparticles in immersion

In a colloidal suspension, the sound damping mechanism strongly depends on the wavevector of the excited acoustic waves [14, 18–22] which, in a scattering experiment, coincides with the exchanged wavevector Q. At Q values well beyond the hydrodynamic limit, yet smaller than those probed by *IXS*, i.e., in the so-called multiple scattering regime, immersed colloids behave as point scattering sources for the density waves impinging on them. The interference between repeatedly scattered waves causes mutual dephasing, which substantially reduces the lifetime of the dominant acoustic excitations. Although a theoretical description is available to predict the behavior of collective modes when acoustic wavelength $2\pi/Q$ vastly exceeds the colloid diameter, much less is known about the opposite regime, which best describes the cases investigated in all *IXS* measurements. In these situations, it is reasonable to anticipate that elastic heterogeneity plays a significant role. Indeed, the mismatch between the elastic constants of the immersed colloids and the hosting medium originates sound speed fluctuations, which ultimately reduce the coherence of the acoustic mode, shortening its lifetime. A more subtle effect of this heterogeneity arises from the different expansion coefficients of the colloid and the hosting fluid. When a compression-rarefaction (acoustic) wave propagates at the colloid interface, the unmatched expansions of the colloid and the surrounding fluid cause interfacial shear stresses which enhance the system's resistance to sound propagation. Several of our previous measurements [14, 21, 23] suggested that one can significantly enhance sound damping via the immersion of even sparse amounts of nanoparticles (NPs). Indeed, this strategy visibly changes the high-frequency acoustic damping probed, e.g., by *IXS* methods [8, 9]. This damping effect can make barely visible inelastic features arising from sound propagation, as shown by figures, 1 and 2, which respectively refer to the case of NP suspensions in water and glycerol. In both plots, the *IXS* spectrum of the suspension (open circles) is compared to the one of the pure solvent (thick grey line) and the instrumental resolution profile (dot-dashed line). For comparison, all spectral profiles are normalized to the respective maxima. It readily appears that the side shoulders present in the lineshape of the pure liquid medium disappear upon NP immersion.

3 the Bayesian modeling of the lineshape

At this stage, the cause of the inelastic shoulders' disappearance in the suspension spectra, as evidenced by figures. 1 and 2 is still unclear. [15, 16]. In particular, it is

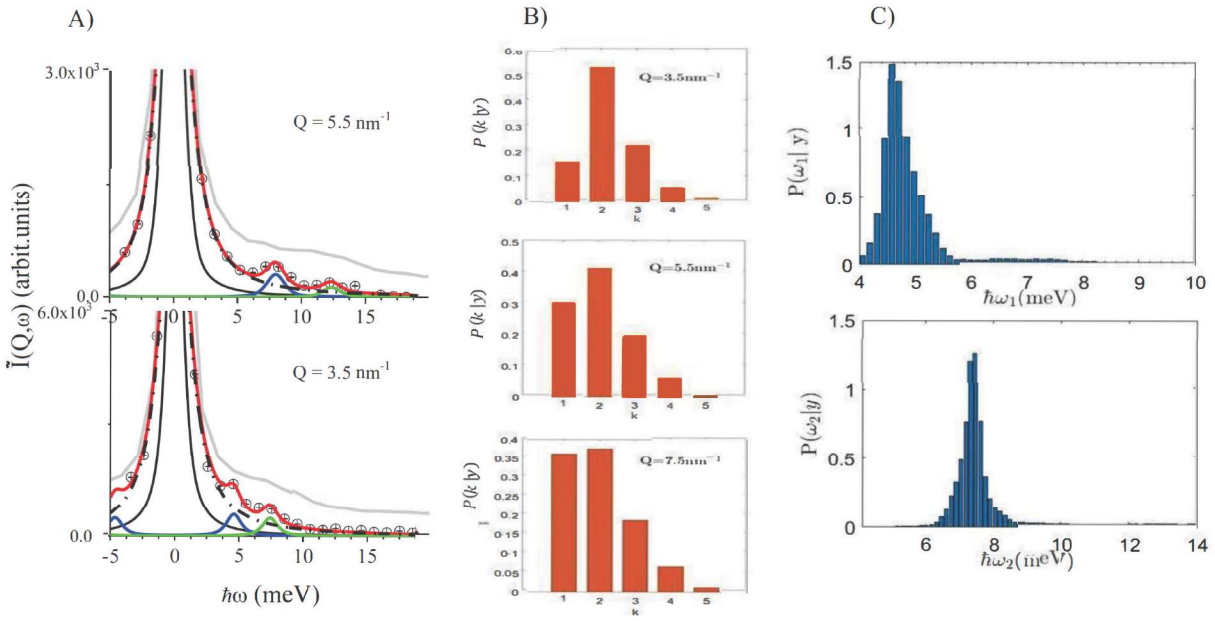

Figure 3. Panel A: the *IXS* spectra from a dilute suspension of Au nanoparticles in water measured at two representative Q's are displayed along with their best fit lineshape and individual spectral components. Panel B: the posterior distribution drawn by the Bayesian inferential algorithm (see text) for the number of inelastic components contributing to the spectral shape is reported for three Q values. Panel C: the posteriors of the inelastic shift of the two phonon modes are displayed as obtained from the Bayesian lineshape analysis of the $Q = 3.5$ nm^{-1} spectrum.

still questionable whether this effect is due to the increase in the damping (width) of inelastic mode, its attenuation (relative amplitude decrease), or the combined effects. Detailed lineshape modeling is the only option to unravel this query properly. A difficulty hampering this endeavor is the lack of a firm analytical prediction for the lineshape in the dynamic ($Q\omega$) range of interest which suggests the use of suitable phenomenological *ansatz*. The latter entails, for instance, the choice of the most plausible number of spectral modes, their shape, their possible coupling with multiple timescale relaxation phenomena, and so forth. Within the approximation eventually adopted, the Q-dependence of shape parameters is determined *a posteriori* only by best-fitting the model to the spectra measured at various Q's. This result is usually achieved through a conventional chi-square minimization routine, whose outcome strongly depends on the *ansatz* adopted. Also, the hybrid, solid-liquid character of a liquid suspension adds further complexity to the interpretation of the spectral shape. To sort out this puzzling scenario, a minimal requirement is to limit the inherent bias of the adopted modeling while opting for an evidence-based analysis of experimental results. The strategy adopted should clarify:

(1) how accurately competitive models account for the measured scattering profiles; (2) how investigators should cope with the opposite risks of "confirmation bias" and data over-interpretation (3) how to circumvent common shortcomings of chi square-based approaches as the convergence to local, rather than global, minima, and, most importantly, (4) how to implement minimally invasive external constraints without wasting information from prior knowledge (if any) of the problem at hand, and (5) how to efficiently handle the limited statistical accuracy of experimental results by enhancing the inferential power of data analysis [24].

Bayesian inferential methods successfully address all these concerns. Furthermore, when applied to the analysis of spectroscopic results, these methods can enable probabilistic hypothesis tests involving, for instance, the number of inelastic modes most likely to appear in the spectrum or the number of relaxation phenomena coupling with them. These unknown numbers can be treated as parameters in the inference procedure. Even more interesting is the possibility of submitting to a hypothesis test the number of relaxations associated with the observed dynamics and the analytic expression that best describes the available data. A very instructive example, not discussed in this short review because it refers to a time scale different from the one tackled here, is provided in Ref. [25]. The inferential analysis performed in this work estimates the number of relaxation channels affecting the time correlation function of an NP aqueous solution, also unraveling the physical nature of such decay channels. Of course, the choice of the model involves a narrow range of options, in this case, limited to combinations of simple exponentials, stretched exponentials, mixtures of stretched and unstretched exponentials, or a simple Kohlrausch–Williams–Watts function [26]. Bayesian methods have already been successfully exploited to extract accurate structure factor amplitudes from a powder diffraction pattern with strongly overlap-

ping Bragg peaks [27]. In other studies [14, 17, 22, 28], they were employed to determine how many excitations are present in an inelastic neutron or X-Ray scattering spectrum. Another application is the determination of the number of diffusive processes affecting the density correlation function in the frequency [29, 30] or in the time domain [25]. The inferential method uses a numerical algorithm based on a Markov Chain Monte Carlo (MCMC) [31] routine with reversible jump (RJ) [32] steps. This numerical routine eventually delivers the joint posterior probability distribution, or simply the posterior, of each model parameter, which represents the best guess on the parameter probability distribution given the experimental evidence and the *a priori* knowledge of the physical problem at hand. The maximum of such a posterior can be naturally interpreted as the most plausible, or best-fitting, value of the parameter involved, provided the posterior profile is sharply peaked, well-shaped, and unimodal. The posterior shape bears direct insight into the uncertainty associated with the best-fitting value. Further details on the Bayesian approach are given in Refs. [17, 25, 33, 34]. The typical outcome of this inferential analysis, when applied to the modeling of the *IXS* spectra from a nanoparticle suspension, is summarized by figure 3, which displays results discussed in Ref. 14. In Panel A of such a figure, we compare the *IXS* spectra from an aqueous suspension of gold NPs with the corresponding best-fitting model lineshapes and their individual spectral components. Panel B shows that the relative probability of the most plausible model option ($k = 2$) decreases upon Q increase, while the probability of the alternative model option ($k = 1$) instead increases. In Ref. 14, the two dominant modes corresponding to the most plausible model option are assigned to the longitudinal (LA) and transverse acoustic (TA) phonons propagating in the Au NP interior. This interpretation primarily rests on two main observations: 1) the maximum values of the dispersion curves of the modes - roughly attained at the edge of the first Brillouin zone - are consistent with the lower and higher frequency maxima of the Au phonon Density of States. Furthermore, the LA dispersion is compatible with the one reported in the literature for liquid gold [35] and 2) The width of these phonon excitations is far narrower than the typical inelastic linewidth of a generic liquid, particularly the one of the hosting liquid (water). In summary, figure 3 indicates that the intra-NP phonons are the only inelastic excitations identifiable by the model in the measured spectral shape of the suspension, despite the NPs being present in it in a very sparse amount (about 0.1 % in volume). This evidence unveils the nearly complete vanishing of collective modes in the hosting liquid. Again, it seems still unclear the phenomenology underlying this disappearance. The results of the Bayesian analysis of our previous IXS measurements [36, 37] reported in figure 4 shed light on this aspect. In particular, Panels A and B of figure 4 display respectively the Q-dependence of the acoustic damping Γ and the ratio A_{in}/A_{tot} between the inelastic component and the total amplitude of the spectrum. Open circles and dots refer to a dilute Au NP suspension in glycerol and to pure glycerol respectively. Panels A and B shows that for $Q \leq 2.5$ nm^{-1} the sound mode in the suspension has smaller amplitude, while for 2.5 nm$^{-1} \leq Q \leq 4.5$ nm^{-1} it has larger damping. A quantitative assessment of the relative lifetime of the longitudinal acoustic mode came from a comparison between its dominant frequency Ω and damping coefficient Γ via the ratio $R = \Omega/\Gamma$. From a physical point of view, the parameter R measures the oscillations experienced by the sound wave before being completely damped off. In Panel C of figure 4, this ratio is reported as a function of Q as obtained from the lineshape modeling of our *IXS* measurements in Ref. 37 on aqueous suspensions of vitreous silica (v-SiO_2) NPs of various sizes and concentrations, either neutral, positively, or negatively charged. The trends shown suggest that the immersion of v-SiO_2-NPs causes the longitudinal mode of the liquid to approach the critical damping condition $\Omega_2/\Gamma_2 = 1$, i.e., visibly reduces its relative lifetime. However, based on the plot, it seems still unclear if and to what extent this damping effect depends on the v-SiO_2 NP characteristics or their relative concentration.

4 New excitations in the dynamics of a suspension

In a series of *IXS* measurements on a dilute (< 1 % volume concentration) suspension of Au NP in glycerol [21] we gain evidence for a low-frequency inelastic mode never observed in the previous investigations on pure glycerol [38–41]. The complete characterization of this spectral mode largely owes to the discussed Bayesian inferential approach, as its presence was often partially hidden by the Lorentzian wings of the instrumental resolution profile. Two relevant aspects of this additional mode, i.e., its spectral fingerprints and dispersive behavior, are illustrated in the two plots of figure 5. This additional spectral feature was, of course, connected with the immersed NPs, and resembled the one previously reported by Brillouin Light Scattering investigations of the hydrodynamic spectrum from colloidal suspensions [18–20]. We assigned this spectral mode to Stoneley waves [42] propagating on the external surface of immersed NPs. Stoneley waves are surface vibrations that primarily propagate at the interface between a liquid and a solid medium as their amplitude rapidly vanishes away from such a boundary. Its propagation velocity is lower than the sound velocities of the solid and liquid media.

As illustrated in figure 5, this low-frequency mode (red squares) coexists with the longitudinal mode of glycerol (open circles) and exhibits a distinctive dispersion behavior characterized by a slow linear Q-increase over an impressively large range of distances $\approx Q^{-1}$, which extends down to mesoscopic scales, while showing no evidence for the Q oscillations typically arising from the interaction with the local arrangement of the liquid. Most importantly, its propagation speed, derived from the slope of its linear Q-trend, is about 520 m/s, i.e., much lower than the sound velocities of glycerol and gold, as to be expected for a Stoneley wave. The cascade of *IXS* spectra in the left panel of figure 5 shows that the spectral contribution of

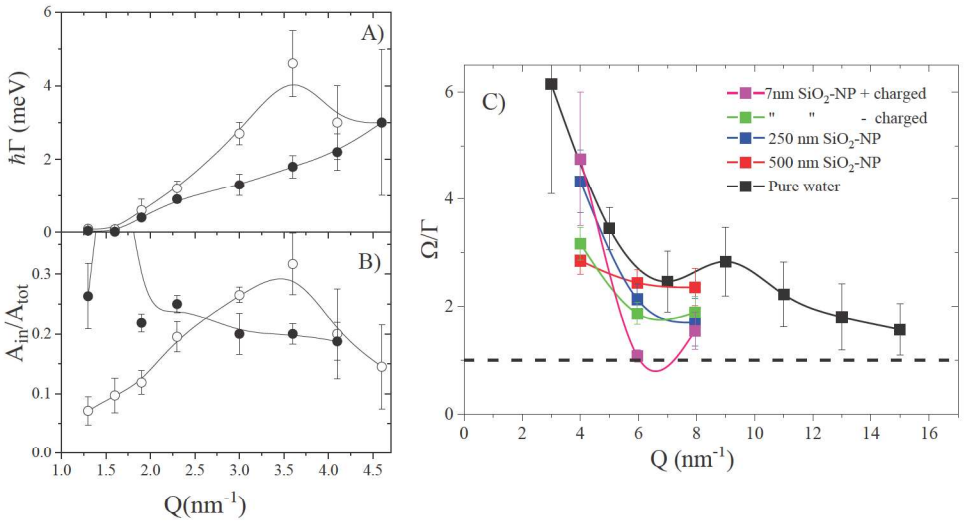

Figure 4. Panel A: The damping coefficient of the collective mode in the spectrum of an Au-NP suspension in glycerol (open circles) is compared with its counterpart in pure glycerol (black dots) as derived from Ref. 36. Solid lines through the data are spline included for visualization purposes. Panel B: The relative amplitude of the inelastic components of the *IXS* spectra, referring to the same measurement and with the same symbols as in panel A. Panel C: The ratio Ω/Γ representing the relative lifetime of the inelastic mode is reported as a function of Q, as obtained from the *IXS* measurements on amorphous SiO_2 NPs of various sizes, either neutral, positively, or negatively charged, as indicated in the legend. Data are from Ref. 37. The dashed horizontal line represents the critical damping condition.

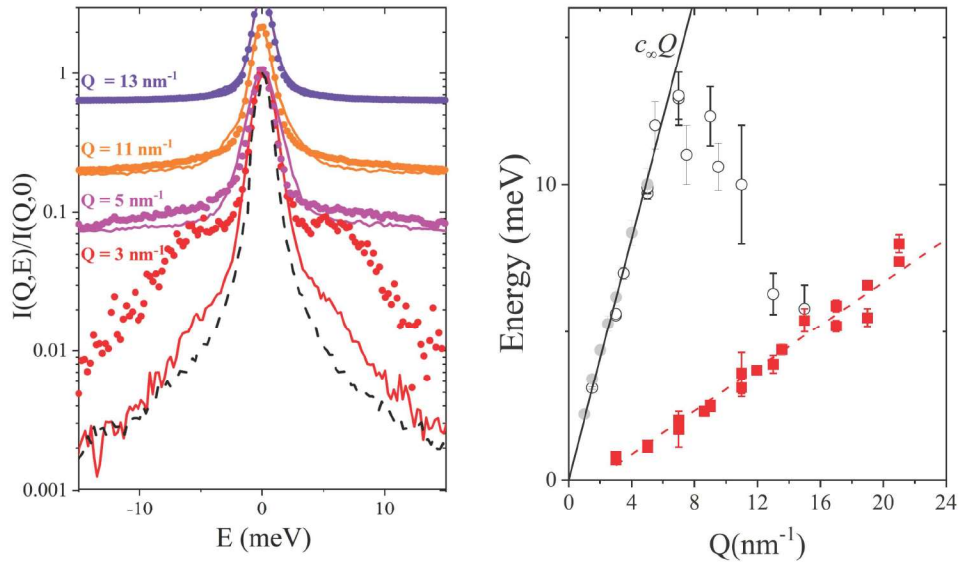

Figure 5. Left panel: *IXS* spectra measured at the indicated Q values in glycerol (dots) and on a dilute Au NP suspension in glycerol (solid lines of the corresponding color). All lineshapes are normalized to the respective intensity maxima and vertically offset for clarity. Right panel: Q dependence of the longitudinal acoustic frequency in both glycerol and pure suspension (open circles) is compared with the low-frequency dispersive branch (red squares) ascribed to Stoneley waves (see text). The solid straight line represents the high-frequency linear dispersion of glycerol (corresponding to a 3100 m/s sound speed) as derived from Ref. 38. The dashed red line is the linear best fit of the low-frequency dispersion branch and has a slope of 520 m/s. Gray dots represent the sound dispersion of pure glycerol reported by Sette and collaborators [39].

this Stoneley mode, albeit somewhat elusive at first sight, consists in a seemingly quasielastic broadening of the central peak in the spectrum. Such a broadening emerges by comparing the scattering profiles of the solution with the one of the pure substrate.

5 The anisotropic dynamics of water under highly directional confinement

Steering acoustic propagation in isotropic systems as fluids is far from trivial as density waves propagating in these systems are much shorter-lived than their counterparts in crystalline materials, and their propagation has no preferential directions. The achievement of this task likewise entails containing the liquid inside highly directional, nanometer-sized cavities. Carbon nanotubes (CNTs) seem ideally suited to this scope as they can act as quasi-unidimensional flow channels for the liquid confined in their interior. In particular, confinement in CNTs is known to drastically modify the physical properties of embedded water [43] as its dipolar configuration [44, 45] and orientational relaxation [46]. Furthermore, when trapped inside CNTs, water exhibits a non-trivial temperature evolution [47, 48]. In this scenario, it seems especially interesting the hypothesis that a highly directional confinement of a liquid may cause an "isotropy breach" of its sound propagation properties. To clarify this point, we conducted an *IXS* study on hydrated multi-walled aligned carbon nanotubes "forest-grown" on a Si substrate [22]. We conducted our measurements with the exchanged wavevector in either the basal or the axial directions of CNTs, these scattering geometries being here referred to as $\boldsymbol{Q}_\perp$ and $\boldsymbol{Q}_\parallel$, respectively.

Such a measurement demonstrates that the water dynamics under this quasi-1D confinement is strongly anisotropic. In particular, we observed that the $\boldsymbol{Q}_\perp$ *IXS* spectrum of hydrated CNTs is dominated by a low-frequency inelastic feature resembling the well-known transverse acoustic mode of water. At the same time, no signatures of collective dynamics appear in the $\boldsymbol{Q}_\parallel$ spectrum. This finding suggests that aligned CNTs visibly affect the propagation of terahertz acoustic modes of water embedded in their interior by acting either as "polarization filters" ($\boldsymbol{Q}_\perp$ geometry) or "acoustic dampers" ($\boldsymbol{Q}_\parallel$ geometry). This finding might inspire the use of these devices to efficiently shape terahertz collective excitations, which is deemed to impact the emerging domain of terahertz phononics. The polarization filtering ability of hydrated CNT is schematically illustrated in figure 6. Panel A displays a Transmission Electron Microscopy image of the forest-grown CNT array we used in Ref. 22 while showing the CNT axis and the perpendicular direction of the wavevector ($\boldsymbol{Q}_\perp$ geometry). Panel B compares the sound dispersion of the only inelastic mode surviving in the $\boldsymbol{Q}_\perp$ spectrum of the hydrated sample and its counterpart in bulk water. The overall agreement between the two curves indicates that orienting the hydrated sample in the $\boldsymbol{Q}_\perp$ scattering geometry selectively enables the propagation of the transverse acoustic mode of water. We finally stress that IXS measurements of the phonon spectrum are not the only characterization tool of the phonon response of a system, a valuable alternative being Inelastic Neutron Scattering. This technique has the undoubted advantage of a substantially narrower and sharper energy resolution profile, as required for a detailed study of low-frequency collective modes gathering in the quasielastic portion of the spectrum. Aside from the direct measurement of the phonon spectrum, neutron scattering can shed insight into the phonon Density of States, possibly revealing its signatures of a non-trivial phonon response. In this perspective, it is worth mentioning recent joint Inelastic Neutron Scattering (INS) measurements and Density Functional Theory ab initio computations on NP superlattices evidencing the increasing visibility of the inter-NP phonon dynamics at low temperatures [50].

6 Perspectives

The results discussed in this brief review are intended as very preliminary steps in a field of research still in its infancy, which essentially consists of the shaping of terahertz sound propagation via the design of the nanoscale structure. The extension of the domain of sound propagation engineering to this uncharted high-frequency territory appears especially compelling, because terahertz phonons are the leading conveyors of heat in insulators, and their control is crucial to implement heat flow management. Perhaps the most encouraging aspect of the whole body of results discussed here is the evidence that visible changes in the sound propagation can be simply achieved by slightly perturbing its internal structure through the immersion of a sparse amount of nanoparticles. Yet these results are only preliminary, and there is still a long distance keeping us apart from the ultimate goal of terahertz sound control. As mentioned in the introductory section, to pursue this objective seems particularly promising the arrangement of nanoparticles in superlattices functioning as the so-called phononic crystals. The density and elastic moduli distribution of these devices has periodicity that interferes directly with sound propagation at some frequency, potentially enabling its full shaping. Any advance in this field critically depends on the joint use of world-class nanotechnology to produce novel samples and spectroscopic methods to characterize their terahertz phonon behavior. Our group has recently become very active in this new field, and this will hopefully soon enable us to share this excitement with the broad community of Condensed Matter physicists.

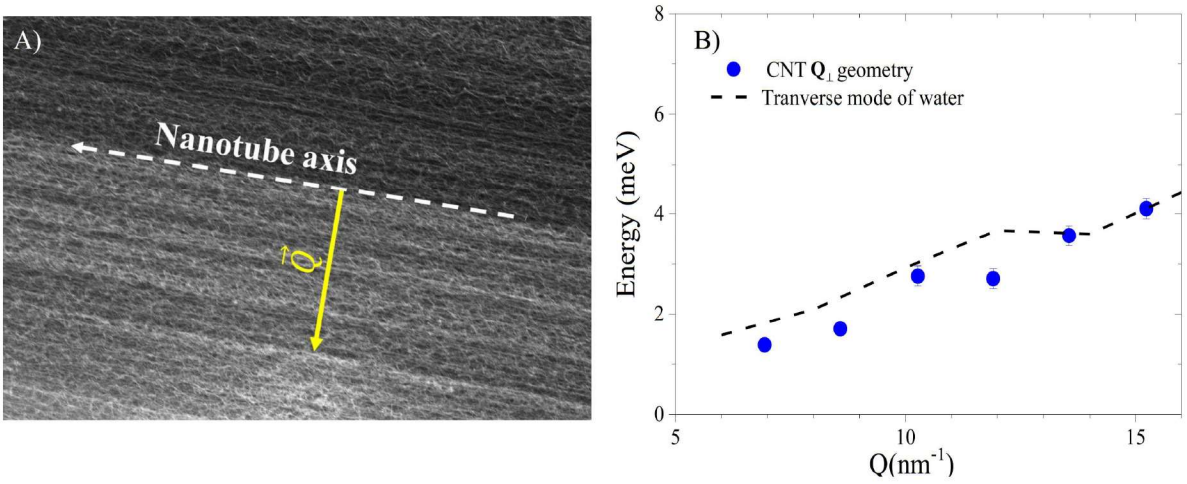

Figure 6. Panel A: Transmission Electron Microscopy image of the forest-grown carbon nanotube (CNT) array used in the *IXS* measurements in Ref. 22, in which the direction of the exchanged momentum and the CNT axis are specified. Panel B: The dispersion curve derived from the inelastic shift of the low-frequency mode in the $\boldsymbol{Q}_\perp$ *IXS* spectra of the hydtrated sample is compared with the Q dispersion of the transverse mode of pure water as derived from Ref. 49 (dashed line).

References

[1] M. Maldovan, Nature **503**, 209 (2013)
[2] Z. Liu, X. Zhang, Y. Mao, Y. Zhu, Z. Yang, C.T. Chan, P. Sheng, science **289**, 1734 (2000)
[3] C.W. Chang, D. Okawa, A. Majumdar, A. Zettl, Science **314**, 1121 (2006)
[4] T. Harman, P. Taylor, M. Walsh, B. LaForge, science **297**, 2229 (2002)
[5] M. Maldovan, Physical review letters **110**, 025902 (2013)
[6] H. Lv, X. Tian, M.Y. Wang, D. Li, Applied Physics Letters **102**, 034103 (2013)
[7] P.E. Hopkins, C.M. Reinke, M.F. Su, R.H. Olsson III, E.A. Shaner, Z.C. Leseman, J.R. Serrano, L.M. Phinney, I. El-Kady, Nano letters **11**, 107 (2011)
[8] A. Cunsolo, *The THz dynamics of liquids probed by inelastic X-ray scattering* (World Scientific, 2021)
[9] S.K. Sinha, Journal of Physics: Condensed Matter **13**, 7511 (2001)
[10] S.W. Lovesey, *Theory of Neutron Scattering from Condensed Matter. Vol. 1: Nuclear Scattering* (Oxford, 1984)
[11] G.L. Squires, *Introduction to the theory of thermal neutron scattering* (Courier Corporation, 1996)
[12] V.M. Giordano, G. Monaco, Proceedings of the National Academy of Sciences **107**, 21985 (2010)
[13] V.M. Giordano, G. Monaco, Physical Review B **84**, 052201 (2011)
[14] A. De Francesco, L. Scaccia, M. Maccarini, F. Formisano, Y. Zhang, O. Gang, D. Nykypanchuk, A.H. Said, B.M. Leu, A. Alatas et al., ACS Nano **12**, 8867 (2018)
[15] A. Gelman, J.B. Carlin, H.S. Stern, D.B. Dunson, A. Vehtari, D.B. Rubin, *Bayesian data analysis* (Chapman and Hall/CRC, 2013)
[16] D. Sivia, J. Skilling, *Data analysis: a Bayesian tutorial* (OUP Oxford, 2006)
[17] A. De Francesco, E. Guarini, U. Bafile, F. Formisano, L. Scaccia, Physical Review E **94**, 023305 (2016)
[18] J. Liu, L. Ye, D. Weitz, P. Sheng, Physical Review Letters **65**, 2602 (1990)
[19] R. Penciu, G. Fytas, E. Economou, W. Steffen, S. Yannopoulos, Physical Review Letters **85**, 4622 (2000)
[20] L. Ye, J. Liu, P. Sheng, D. Weitz, Physical Review E **48**, 2805 (1993)
[21] A. De Francesco, L. Scaccia, F. Formisano, E. Guarini, U. Bafile, M. Maccarini, A. Alatas, Y.Q. Cai, D. Nykypanchuk, A. Cunsolo, Physical Review E **102**, 022601 (2020)
[22] A. De Francesco, L. Scaccia, F. Formisano, M. Maccarini, F. De Luca, A. Parmentier, A. Alatas, A. Suvorov, Y.Q. Cai, R. Li et al., Physical Review B **101**, 054306 (2020)
[23] A.D. De Francesco, L. Scaccia, F. Formisano, E. Guarini, U. Bafile, M. Maccarini, A. Alatas, Y.Q. Cai, A. Cunsolo, Nanomaterials **10**, 860 (2020)
[24] D.V. Lindley, Teach. Stat. **15**, 22 (1993)
[25] A. De Francesco, L. Scaccia, R.B. Lennox, E. Guarini, U. Bafile, P. Falus, M. Maccarini, Phys. Rev. E **99**, 052504 (2019)
[26] G. William, D.C. Watts, Transac. Faraday Soc. **66**, 80 (1970)
[27] D. Sivia, W. David, Acta Crystallogr. A **50**, 703 (1994)
[28] A. De Francesco, U. Bafile, A. Cunsolo, L. Scaccia, E. Guarini, Scientific Reports **11**, 1 (2021)
[29] D. Sivia, W. Hamilton, G. Smith, Physica B **173**, 121 (1991)

[30] L. Pardo, M. Rovira-Esteva, S. Busch, M. Ruiz-Martin, J.L. Tamarit, T. Unruh, arXiv preprint arXiv:0907.3711 (2009)

[31] W.R. Gilks, S. Richardson, D.J. Spiegelhalter, *Markov chain Monte Carlo in practice* (Chapman & Hall/CRC, 1996)

[32] P.J. Green, Biometrika **82**, 711 (1995)

[33] A. De Francesco, A. Cunsolo, L. Scaccia, in *Inelastic X-Ray Scattering and X-Ray Powder Diffraction Applications*, edited by A. Cunsolo, M.K.K.D. Franco, F. Yokaichiya (IntechOpen, 2020), chap. 2, p. 26

[34] A. De Francesco, L. Scaccia, M. Maccarini, F. Formisano, E. Guarini, U. Bafile, A. Cunsolo, Materials **12**, 2914 (2019)

[35] E. Guarini, S. Bellissima, U. Bafile, E. Farhi, A. De Francesco, F. Formisano, F. Barocchi, Physical Review E **95**, 012141 (2017)

[36] A. De Francesco, F. Formisano, L. Scaccia, E. Guarini, U. Bafile, M. Maccarini, D. Nykypanchuck, A. Suvorov, Y.Q. Cai, S.T. Lynch et al., Nanomaterials **12**, 2401 (2022)

[37] A. De Francesco, L. Scaccia, F. Formisano, E. Guarini, U. Bafile, M. Maccarini, Y. Zhang, D. Nykypanchuck, A. Alatas, A. Cunsolo, Scientific Reports **11**, 1 (2021)

[38] A. Cunsolo, B. Leu, A. Said, Y. Cai, The Journal of chemical physics **134**, 184502 (2011)

[39] F. Sette, M.H. Krisch, C. Masciovecchio, G. Ruocco, G. Monaco, Science **280**, 1550 (1998)

[40] C. Masciovecchio, G. Baldi, S. Caponi, L. Comez, S. Di Fonzo, D. Fioretto, A. Fontana, A. Gessini, S.C. Santucci, F. Sette et al., Physical Review Letters **97**, 035501 (2006)

[41] A. Giugni, A. Cunsolo, Journal of Physics: Condensed Matter **18**, 889 (2006)

[42] R. Stoneley, Proceedings of the Royal Society of London. Series A, Containing Papers of a Mathematical and Physical Character **106**, 416 (1924)

[43] B. Mukherjee, P.K. Maiti, C. Dasgupta, A. Sood, ACS nano **4**, 985 (2010)

[44] J. Köfinger, G. Hummer, C. Dellago, Proceedings of the National Academy of Sciences **105**, 13218 (2008)

[45] C. Cametti, F. De Luca, A. Parmentier, The Journal of Chemical Physics **137**, 094908 (2012)

[46] B. Mukherjee, P.K. Maiti, C. Dasgupta, A.K. Sood, Acs Nano **2**, 1189 (2008)

[47] A.I. Kolesnikov, J.M. Zanotti, C.K. Loong, P. Thiyagarajan, A.P. Moravsky, R.O. Loutfy, C.J. Burnham, Physical review letters **93**, 035503 (2004)

[48] G. Briganti, G. Rogati, A. Parmentier, M. Maccarini, F. De Luca, Scientific reports **7**, 1 (2017)

[49] A. Cunsolo, C. Kodituwakku, F. Bencivenga, M. Frontzek, B. Leu, A. Said, Physical Review B **85**, 174305 (2012)

[50] N. Yazdani, M. Jansen, D. Bozyigit, W.M. Lin, S. Volk, O. Yarema, M. Yarema, F. Juranyi, S.D. Huber, V. Wood, Nature communications **10**, 1 (2019)